



TITLE:

Molecular Dynamics Simulation of Structure of Liquid Methane

AUTHOR(S):

Oobatake, Motohisa; Hayashi, Soichi; Machida, Katsunosuke

CITATION:

Oobatake, Motohisa ...[et al]. Molecular Dynamics Simulation of Structure of Liquid Methane. Bulletin of the Institute for Chemical Research, Kyoto University 1990, 68(4): 255-264

ISSUE DATE:

1990-12-30

URL:

<http://hdl.handle.net/2433/77348>

RIGHT:

Molecular Dynamics Simulation of Structure of Liquid Methane

Motohisa OOBATAKE*, Soichi HAYASHI** and Katsunosuke MACHIDA***

Received September 19, 1990

Molecular dynamics simulation has been used to investigate the radial distribution, diffusion constant, and trajectories of molecules for liquid methane. The simulation reproduced well the C··C radial distribution obtained from X-ray diffraction experiment. The C··H and H··H radial distributions indicate that hydrogen atoms tend to avoid each other and molecules orient in such a manner as a gear wheel. The self-diffusion coefficient evaluated from this simulation agrees satisfactorily with the value obtained from NMR experiment. Cooperative rotational motion and over-all translation are observed from comparing between the trajectories in a space fixed coordinate system and in a molecular fixed coordinate system.

KEY WORDS: Molecular dynamics/ Liquid methane/ Radial distribution/ Diffusion constant/ Dynamic structure

INTRODUCTION

Molecular dynamics simulation has been used to know the time dependent and average quantities of liquid. In the previous simulation studies^{1,2)}, methane molecule was treated as a rigid body. However, in order to reproduce more precise structure, methane molecule should be represented by a flexible molecule, i.e., inclusion of bond stretching and valence angle bending. Using this flexible molecule, infrared and Raman spectra of small compounds such as sulfur dioxide³⁾, benzoic acid crystal⁴⁾, and molten LiNO₃⁵⁻⁷⁾ were calculated.

In order to represent the interaction between methane molecule, Hanley and Watts¹⁾ used isotropic m-6-8 potential, while Murad *et al.*²⁾ used anisotropic exponential-6 model proposed by Williams⁸⁾ who determined the parameters of Van der Waals interaction for C and H from crystal lattice energies of several hydrocarbons. Determination of atomic potential parameter directly from methane molecules⁹⁾ was done by using the value of the second virial coefficient of methane molecule, in which interaction was separated into three kinds of combinations of constituent atoms C and H. In this study, this potential function was used for the simulation to compare with the other potential function.

In this paper, radial distribution between constituent atoms of methane molecule and dynamic properties such as diffusion constant and trajectories of center of mass were obtained by the molecular dynamics simulation technique including

* 大畠玄久: Protein Engineering Research Institute, 6-2-3 Fuedai, Suita, Osaka 565, Japan

** 林 宗市: Laboratory of Surface Chemistry, Institute for Chemical Research, Kyoto University, Uji, Kyoto 611, Japan

*** 町田勝之輔: Faculty of Pharmaceutical Sciences, Kyoto University, Kyoto 606, Japan

all degrees of freedom.

METHOD

The simulation is performed by the same method as used for liquid sulfur dioxide in a previous work³⁾. We consider a system of N atoms interacting through intra- and intermolecular potentials in the condition of microcanonical ensemble. The force F_i on the i th atom is represented by the sum of the intra- and intermolecular forces, F_i^{intra} and F_i^{inter} ,

$$\begin{aligned} F_i &= F_i^{intra} + F_i^{inter} \\ &= -\frac{\partial V^{intra}}{\partial \mathbf{r}_i} - \frac{\partial V^{inter}}{\partial \mathbf{r}_i}, \quad i=1, \dots, N \end{aligned} \quad (1)$$

where V^{intra} and V^{inter} are the intra- and intermolecular potential energies, respectively, and \mathbf{r}_i is the position vector whose components are along the space-fixed Cartesian coordinate system.

The intramolecular potential energy V^{intra} is expressed in terms of the internal coordinates as

$$\begin{aligned} V^{intra} &= \frac{1}{2} \sum_{tt'} f_{tt'} S_t \cdot S_{t'} + \frac{1}{6} \sum_{tt't''} g_{tt't''} S_t \cdot S_{t'} \cdot S_{t''} + \frac{1}{24} \sum_{tt't''t'''} h_{tt't''t'''} S_t \cdot S_{t'} \cdot S_{t''} \cdot S_{t'''} \\ &\quad S_t \cdot S_{t'} \cdot S_{t''} \cdot S_{t'''} \end{aligned} \quad (2)$$

where $f_{tt'}$, $g_{tt't''}$, and $h_{tt't''t'''}$ are the quadratic¹⁰⁾, cubic, and quartic force constants¹¹⁾, respectively, which are listed in Table I and S_t , $S_{t'}$, $S_{t''}$, and $S_{t'''}$ are t th, t' th, t'' th, and t''' th internal coordinates, respectively.

Table I. Force constants of methane.

	Force constant
K (r_i, r_i)	5.495
K (r_i, r_j)	0.124
K (ϕ_i, ϕ_i)/l ²	0.548
K (ϕ_i, ϕ_j)/l ²	-0.0185
K (r_i, ϕ_i)/l	0.165
K (r_i, r_i, r_i)	-31.466
K (r_i, r_i, r_i, r_i)	173.0

Units are aJÅ⁻², aJÅ⁻³, and aJÅ⁻⁴ for quadratic, cubic, and quartic force constants, respectively.

The intermolecular potential energy V^{inter} is expressed in terms of the sum of the pairwise atom-atom potential,

$$V^{inter} = \sum_{ij} (-A r_{ij}^{-6} + B r_{ij}^{12}) \quad (3)$$

where r_{ij} is the distance between atoms i and j and A and B are attractive and repulsive parameters, respectively⁹⁾. These values are listed in Table II with the minimum energy E_{min} at the distance r_{min} . This Lennard-Jones 6-12 potential energy⁹⁾ which was determined directly from the value of the second virial coefficient

Table II. Lennard-Jones atom-atom potential parameters.

Atomic pair	A/aJÅ ⁶	B/aJÅ ¹²	$r_{min}/\text{Å}$	$E_{min}/10^{-4} \text{ aJ}$
C-C	4.028	8248.9	4.0	-4.92
C-H	0.868	560.5	3.3	-3.36
H-H	0.188	28.968	2.6	-3.05

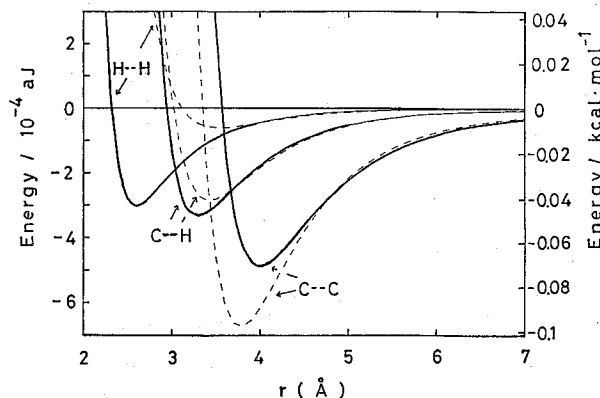


Fig. 1. The potential function for C··C, C··H and H··H for Lennard-Jones⁹⁾ (—) and Buckingham potential function⁹⁾ (---), respectively. Unit of energy is aJ=144 kcal/mol.

cient of methane molecule is shown in Fig. 1, comparing with a potential of set VII in Table I of Williams⁸⁾ used by Narten *et al.*¹²⁾. Both potential energy curves resemble each other for C··H and C··C interactions but for H··H, i.e., the former has more deep energy ($E_{min} = -3.05 \cdot 10^{-4} \text{ aJ}$) at shorter equilibrium distance ($r_{min} = 2.6 \text{ Å}$) than the latter ($E_{min} = -0.7 \cdot 10^{-4} \text{ aJ}$ and $r_{min} = 3.74 \text{ Å}$). The forces acting on an atom have been assumed pairwise up to cut off distances 8.6, 7.2, and 5.6 Å for C··C, C··H, and H··H, respectively, where the energy at the distance is $E_{min}/50$. In order to reduce the error resulting from this truncation, the shifted force potentials were adopted¹³⁾.

We consider a system of 125 CH₄ molecules in a cubic periodic box of length 20.0 Å. This corresponds to density of 0.415 g/cm³. The equilibrium CH bond length and HCH bond angle were adopted as the experimental values of 1.093 Å and 109.5°, respectively. The classical trajectories $r_1(t), \dots, r_N(t)$ were obtained by integrating Newton's second law where a modified Verlet integration algorithm¹⁴⁾ was used with a periodic boundary condition. The time step was set to 1/4096 ps ($\approx 0.244 \text{ fs}$) and total running time was 131 ps where the first 2 ps was discarded for the thermal equilibrium. The calculation was carried out using a FACOM M380Q computer at the Institute for Chemical Research, Kyoto University. The calculation for 1 ps run required 4 hr of the computer. The temperature varied from 94 K of the first 3 ps to 88 K of 95 ps and fluctuates within 3 K during 1 ps run. The average temperature through the simulation was 91 K and the average pressure was -500 atmosphere.

RESULTS AND DISCUSSION

1. Radial distribution function

An experimental radial distribution function for C··C, $g_{cc}(r)$, was determined from the distinct structure function $H_d(k)$ of an X-ray diffraction data for liquid methane at 92 K¹²⁾

$$g_{cc}(r) = 1 + \frac{1}{2\pi^2 r \rho} \int_0^\infty k H_d(k) \sin kr \, dk \quad (4)$$

where ρ is the number density of methane, $k = 4\pi \sin \theta / \lambda$, θ is the Bragg scattering angle, and λ is the radiation wavelength. On the other hand, a calculated radial distribution function from molecular dynamics simulation is given by

$$g_{cc}(r) = \left\langle \frac{1}{N} \sum_{i=1}^N \left[\frac{V}{N} \frac{\Delta n_{cc}(r)}{4\pi r^2 \Delta r} \right] \right\rangle_t \quad (5)$$

where N is the number of C atom in the volume V and Δn_{cc} is the number of C atom in the radius range from $r - \Delta r/2$ to $r + \Delta r/2$. The function $\rho g_{cc}(r)$ is the probability for finding carbon atoms at a distance r from a given carbon atom. Observed and calculated distribution functions are compared with each other in Fig. 2. The calculated distribution function which has maxima at 4.0, 7.5, and 11.0 Å was derived from an average over 1,280 steps during 40 ps starting from 50 ps. Three calculated distribution functions shown in Figs. 3-5 had the same values as those starting from 10 ps indicating good statistics. The agreement between the calculated and experimental distributions is very good with only a small difference at the distance 5.5, 7.5, and 11 Å. These differences were also seen for a reference interaction site model (RISM) by the method of integral equation using Williams

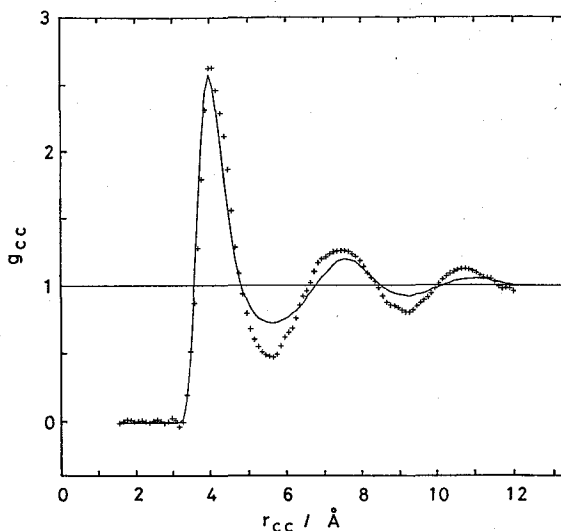


Fig. 2. Radial distribution function of C··C for this molecular dynamics study (—) averaged over 1,280 steps during 40 ps starting from 50 ps and an X-ray diffraction study (+++) at 92 K¹²⁾.

6-exp potential¹²⁾.

The average number of neighbors for methane molecule is obtained from

$$n_{cc} = 4\pi\rho \int_0^R r^2 g_{cc}(r) dr \quad (6)$$

where the upper integration limit R is taken as the position of successive minima in g_{cc} . When we take $R=5.6 \text{ \AA}$, $n_{cc}=11$ which is close to an experimental value $n_{cc}=12^{12)}$. This small difference comes from the difference in number density, i.e., $\rho_{cal}=0.01563/\text{\AA}^3$ is smaller than $\rho_{exp}=0.01702/\text{\AA}^3$.

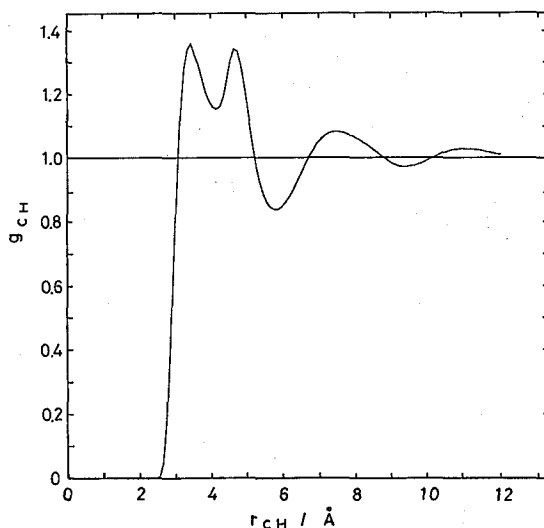


Fig. 3. Average radial distribution function of C··H for this molecular dynamics study during 40 ps at 92 K.

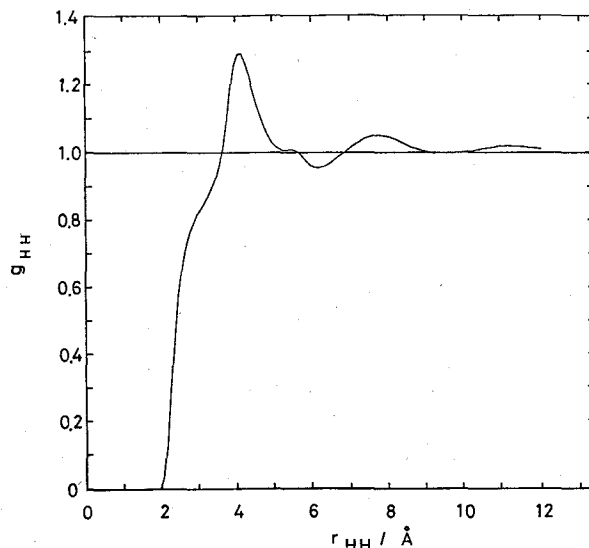


Fig. 4. Average radial distribution function of H··H for this molecular dynamics study during 40 ps at 92 K.

Other distribution functions, g_{CH} and g_{HH} , are calculated by the same method and shown in Fig. 3 and Fig. 4, respectively. The peaks appearing at the distances 3.5 and 4.7 Å for r_{CH} and those at the distances 2.8 and 4.2 Å for r_{HH} suggest the predominant orientation of two interacting molecules. Radial distribution functions evaluated from our flexible molecule with Lennard-Jones potential¹⁹ for C··C, C··H, and H··H gave the similar results to those for rigid body model with Buckingham potential of Williams by Murad *et al.*²⁰. This similar result would come from the similarity of C··H potential for both models and compensation of H··H potential with large r_{min} and shallow E_{min} and C··C potential with deep E_{min} in Williams potential compared to Lennard-Jones potential. If both of methane molecules which closely contact at H atom have the same directions of bond connecting the contact H atom and C atom of a molecule, those peak distances are calculated from the Van der Waals radius (1.3 Å) of hydrogen atom and the bond length r_b (1.093 Å). Fig. 5A shows this model in which the distance r_{CC} is 4.8 Å and the distances r_{CH} are 3.7 Å for the first nearest neighbor and 5.3 Å for the second one. Similarly, the distances r_{HH} between atoms H and H for this structure is given by 2.6, 4.2, and 5.5 Å. These distances for the three distributions of this model are longer than the simulated values. If hydrogen atoms of both molecules is moved to an opposite direction by rotation and the carbon atom approaches each other, each distance is close to the calculated peak. This average structure of two interacting methane molecule which rotate like gear wheel is shown in Fig. 5B.

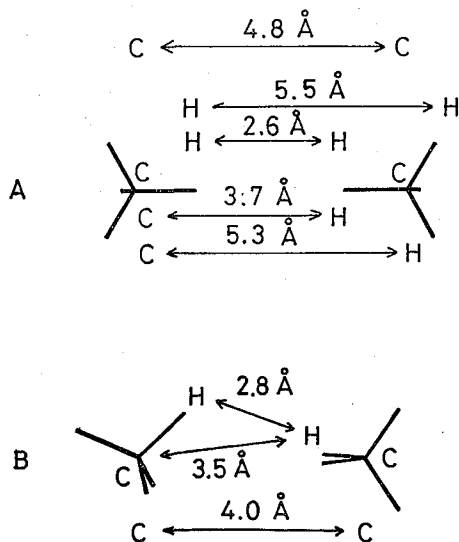


Fig. 5. A. The relative orientation of two methane molecules which has the same direction of bond and closely contacts at H atom. B. The relative orientation of two methane molecules which gives the good correspondence to the simulated radial distribution function for C··C, C··H and H··H.

2. Self-diffusion coefficient

The self-diffusion coefficient D was calculated from the mean squared displacement of the center of mass of a molecule using

$$D = \lim_{t \rightarrow \infty} \frac{1}{6} \langle |r_i(t+t_0) - r_i(t_0)|^2 \rangle. \quad (7)$$

Fig. 6 shows the mean squared displacement against time averaged over 20 scans of 2 ps taken from the first 10 ps at 93 K. From the figure, diffusion constant is estimated as $7.1 \cdot 10^{-5} \text{ cm}^2/\text{s}$. Self-diffusion coefficient for liquid methane obtained by the NMR spin-echo technique was measured at 110, 140 and 160 K¹⁵⁾. It shows that the constant D is proportional to \sqrt{T} and molar volume. Using the molar volume of this study ($38.63 \text{ cm}^3/\text{mol}$) and temperature 93 K, the experimental constant is obtained; $D = 5.7 \cdot 10^{-5} \text{ cm}^2/\text{s}$ which is close to the simulated value.

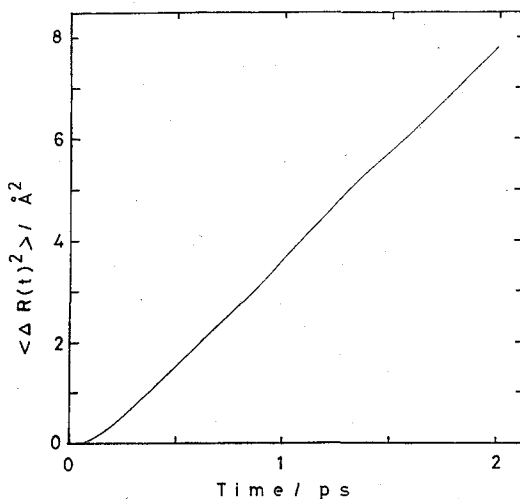


Fig. 6. Mean square distance against time averaged over 20 runs of 2 ps taken from the first 10 ps at 93 K. Self-diffusion constant is obtained from the slope of this line.

3. Trajectory of center of mass

In order to see dynamic behavior of methane molecules, trajectory of a center of mass was investigated in a sliced periodic box normal to the z -axis by 8 \AA . Typical trajectories of one and two ps intervals from the same start are shown in Fig. 7 and Fig. 8, respectively. Mixing of circular and straight movements is seen for each molecule. In order to delete overall translational movement, each molecule is translated to a coordinate system whose origin is fixed at the central molecule, and the whole system is so rotated as to restore the initial orientation of the central molecule. These movements of the molecules from the same start as Fig. 7 and Fig. 8 during one and two ps are plotted as shown in Fig. 9 and 10, respectively. Nearest neighbor molecules show the circular movement around the central molecule as seen by bold lines in Fig. 10. The overall movements are also observed from the large displacement of Fig. 7 compared with Fig. 9. From the results

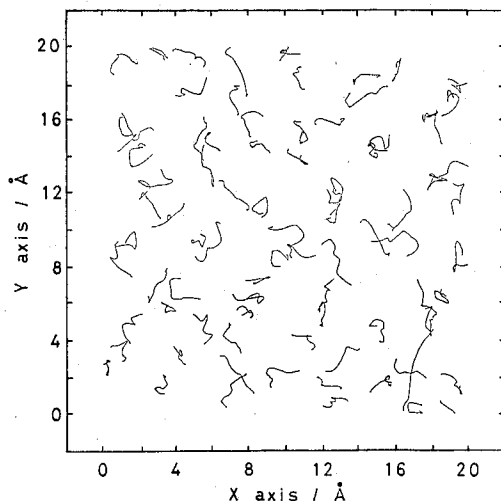


Fig. 7. One ps trajectories of the center of mass from the 60 ps at 90 K. A periodic box is sliced in parallel to xy plane by 8 Å.

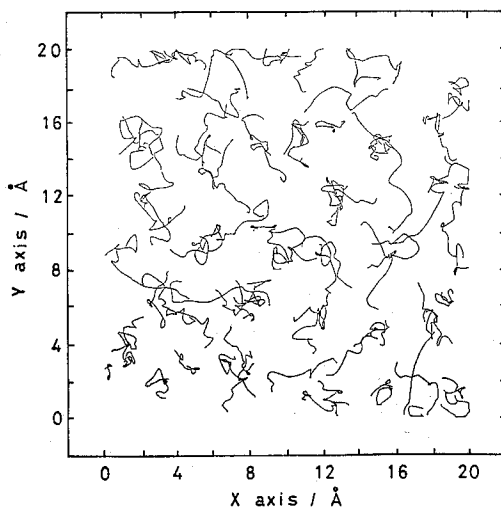


Fig. 8. Two ps trajectories of the center of mass from the 60 ps.

of radial distribution and trajectories, it is suggested that neighboring molecules tend to rotate like gear wheels and push each other toward the low density space.

CONCLUSIONS

The radial distribution and dynamic properties such as diffusion constant and trajectories of center of mass for liquid methane are simulated using molecular dynamics technique. The simulation reproduced well the radial distribution between C··C obtained from an X-ray diffraction experiment. Using the molecular dynamics, radial distribution estimated from our flexible molecule with Lennard-Jones potential for C··C, C··H, and H··H gave similar results with the rigid body model

Molecular Dynamics of Liquid Methane

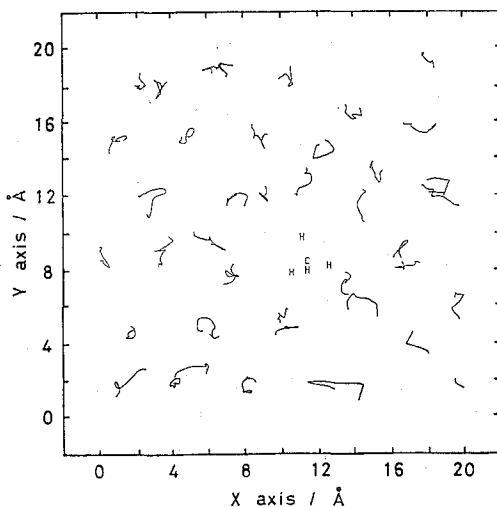


Fig. 9. One ps trajectories of the center of mass from the 60 ps. Movement of molecules seen from a central molecule which is fixed.

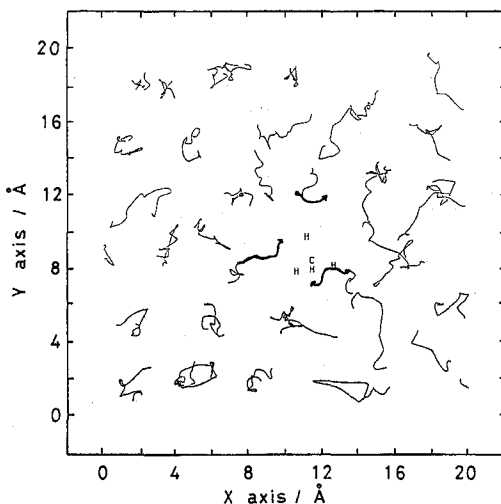


Fig. 10. Two ps trajectories of the center of mass from the 60 ps. Movement of molecules are seen from a central molecule which is fixed. Circular movements around the central molecule from 1 ps to 2 ps are represented by bold lines.

with Buckingham potential of Williams by Murad *et al.*. These radial distributions indicate the preferred orientation of two interacting molecules such as two interacting methane molecules rotating like gear wheel. The self-diffusion coefficient from this dynamics represented the similar value obtained by NMR. Neighboring molecules tend to rotate like gear wheels and push each other toward the low density space. The infrared and Raman spectra simulated in this work will be published elsewhere.

REFERENCES

- 1) H.J.M. Hanley and R.O. Watts, *Mol. Phys.* **29**, 1907-1917 (1975); *Aust. J. Phys.* **28**, 315-324 (1975).
- 2) S. Murad, D.J. Evans, K.E. Gubbins, W.B. Streett and D.J. Tildesley, *Mol. Phys.* **37**, 725-736 (1979).
- 3) S. Hayashi, M. Oobatake, T. Ooi and K. Machida, *Bull. Chem. Soc. Japan* **58**, 1105-1108 (1985).
- 4) R. Nakamura, K. Machida, M. Oobatake and S. Hayashi, *Mol. Phys.* **64**, 215-227 (1988).
- 5) K. Kato, K. Machida, M. Oobatake and S. Hayashi, *J. Chem. Phys.* **89**, 3211-3221 (1988).
- 6) K. Kato, K. Machida, M. Oobatake and S. Hayashi, *J. Chem. Phys.* **89**, 7471-7477 (1988).
- 7) K. Kato, K. Machida, M. Oobatake and S. Hayashi, *J. Chem. Phys.* **92**, 5506-5516 (1990).
- 8) D.E. Williams, *J. Chem. Phys.* **47**, 4680-4684 (1967).
- 9) M. Oobatake and T. Ooi, *Prog. Theor. Physics* **48**, 2132-2143 (1972).
- 10) L.H. Jones and R.S. McDowell, *J. Molecular Spectroscopy* **3**, 632-653 (1959).
- 11) D.L. Gray and A.G. Robiette, *Molecular Physics* **37**, 1901-1920 (1979).
- 12) A. Habenschuss, E. Johnson and A.H. Narten, *J. Chem. Phys.* **74**, 5234-5241 (1981).
- 13) W.B. Streett, D.J. Tildesley and G. Saville, "Computer Modeling of Matter", by P. Lykas, ACS Symposium series (1978), p. 144.
- 14) D. Beeman, *J. Comp. Phys.* **20**, 130-139 (1976).
- 15) K.R. Harris and N.J. Trappeniers, *Physica* **104A**, 262-280 (1980).